



## Analytical Methods

## Near-infrared hyperspectral imaging and partial least squares regression for rapid and reagentless determination of Enterobacteriaceae on chicken fillets

Yao-Ze Feng<sup>a</sup>, Gamal ElMasry<sup>a</sup>, Da-Wen Sun<sup>a,\*</sup>, Amalia G.M. Scannell<sup>b</sup>, Des Walsh<sup>c</sup>, Noha Morcy<sup>a</sup><sup>a</sup> FRCFT Group, School of Biosystems Engineering, University College Dublin, National University of Ireland, Agriculture & Food Science Centre, Belfield, Dublin 4, Ireland<sup>b</sup> School of Agriculture and Food Science, University College Dublin, National University of Ireland, Agricultural & Food Science Centre, Belfield, Dublin 4, Ireland<sup>c</sup> Teagasc Food Research Centre, Ashtown, Dublin 15, Ireland

## ARTICLE INFO

## Article history:

Received 20 March 2012

Received in revised form 11 October 2012

Accepted 8 November 2012

Available online 17 November 2012

## Keywords:

Hyperspectral imaging

Chemical imaging

Food safety

Bacterial pathogens

Enterobacteriaceae

Chemometric

## ABSTRACT

Bacterial pathogens are the main culprits for outbreaks of food-borne illnesses. This study aimed to use the hyperspectral imaging technique as a non-destructive tool for quantitative and direct determination of Enterobacteriaceae loads on chicken fillets. Partial least squares regression (PLSR) models were established and the best model using full wavelengths was obtained in the spectral range 930–1450 nm with coefficients of determination  $R^2 \geq 0.82$  and root mean squared errors (RMSEs)  $\leq 0.47 \log_{10} \text{CFU g}^{-1}$ . In further development of simplified models, second derivative spectra and weighted PLS regression coefficients (BW) were utilised to select important wavelengths. However, the three wavelengths (930, 1121 and 1345 nm) selected from BW were competent and more preferred for predicting Enterobacteriaceae loads with  $R^2$  of 0.89, 0.86 and 0.87 and RMSEs of 0.33, 0.40 and  $0.45 \log_{10} \text{CFU g}^{-1}$  for calibration, cross-validation and prediction, respectively. Besides, the constructed prediction map provided the distribution of Enterobacteriaceae bacteria on chicken fillets, which cannot be achieved by conventional methods. It was demonstrated that hyperspectral imaging is a potential tool for determining food sanitation and detecting bacterial pathogens on food matrix without using complicated laboratory regimes.

© 2012 Elsevier Ltd. All rights reserved.

## 1. Introduction

Meats are highly perishable. In order to maintain good safety record of meats, besides preservation methods such as novel refrigeration processes (Sun & Eames, 1996; Sun, Eames, & Aphornratana, 1996; Sun, 1996, 1997a, 1997b, 1998, 1999), rapid methods for microbial safety detection are also required.

Enterobacteriaceae is a large group of bacteria that are rod-shaped, Gram-negative, facultatively anaerobic and non-spore forming. Microbes from this group ferment sugars to produce acids and gas (Ray, 2000). This group is closely associated with the intestines and faeces of mammals and birds and *Escherichia coli*, *Shigella*, *Salmonella*, *Yersinia* are enteric pathogens that are included in this group. Thus, the amount of Enterobacteriaceae is usually used as a good indicator for food sanitation by accounting for potential faecal contamination and existence of pathogenic bacteria (Olsson, Ahnér, Pettersson, & Molin, 2004). Detection of Enterobacteriaceae bacteria is of significant importance because food-borne illnesses caused by its member pathogens can result in substantial negative influence to the public. Traditional methods, including culture and colony counting methods, polymerase chain reaction (PCR) as well as immunology-based approaches, are

available for precise determination of these microorganisms. However, these methods can be tedious or expensive and require well-trained personnel to carry out experiments due to technical complexity (Velusamy, Arshak, Korostynska, Oliwa, & Adley, 2010) and require 24–72 h to obtain a completed result. Therefore, it is urgently necessary to develop a simple, fast, accurate and non-destructive method for determination of Enterobacteriaceae.

Near infrared spectroscopy (NIRS) is a good technique for indirect and fast detection of biological materials (Chao et al., 2008). It has been successfully employed in detecting bacteria in species (Rodriguez-Saona, Khambaty, Fry, & Calvey, 2001), genus (Alexandrakis, Downey, & Scannell, 2008) and strain (Rodriguez-Saona, Khambaty, Fry, Dubois, & Calvey, 2004; Rodriguez-Saona et al., 2001; Siripatrawan, Makino, Kawagoe, & Oshita, 2010; Suthiluk, Saranwong, Kawano, Numthuan, & Satake, 2008) levels in isolated systems. For direct detection of bacteria on the food matrix, applications were also reported on meat spoilage studies (Alexandrakis, Downey, & Scannell, 2012; Lin et al., 2004), where Alexandrakakis et al. (2012) found that the correct classification of intact chicken breast muscles stored for 8 and 14 days could be ascribed to the increase of free amino acids and peptides over meat storage. Although good performance of NIRS for the detection of bacteria has been verified, the application of NIRS has been greatly restricted. Because the spatial information is absent, NIRS only provides spectral information about the target where one spectrum

\* Corresponding author. Tel.: +353 1 7167342; fax: +353 1 7167493.

E-mail address: [dawen.sun@ucd.ie](mailto:dawen.sun@ucd.ie) (D.-W. Sun).URLs: <http://www.ucd.ie/refrig>, <http://www.ucd.ie/sun> (D.-W. Sun).

is recorded to represent the corresponding sample (Liu, He, Wang, & Sun, 2011; Shao, Bao, & He, 2011; Woodcock, Fagan, O'Donnell, & Downey, 2008). Such deficiency can be overcome by introducing hyperspectral imaging technique (Karimi, Maftoonazad, Ramaswamy, Prasher, & Marcotte, 2012).

By combining spectroscopy with computer vision (Sun, 2000; Sun & Brosnan, 2003; Du & Sun, 2006; Zheng, Sun, & Zheng, 2006a, 2006b), hyperspectral imaging (HSI) is an emerging technology that makes full use of both spectral and spatial information to account for physical, chemical and biological attributes of the samples (ElMasry & Sun, 2010; Menesatti, D'Andrea, & Costa, 2007; Menesatti et al., 2009). It has been widely used in food quality and safety control (Feng & Sun, 2012; Gowen, O'Donnell, Cullen, Downey, & Frias, 2007; Lorente et al., 2012). With respects to bacterial detection, Dubois, Neil Lewis, Fry, and Calvey (2005) proved that HSI was a potential tool for high throughput assay of presence or absence of pathogens in the food matrix by processing the images of isolated microbes. Some other researchers utilised this technology for determination of microbiological spoilage of chicken (Grau et al., 2011), beef (Peng et al., 2011) and pork (Tao et al., 2010; Wang, Peng, & Zhang, 2010). Additionally, Siripatrawan, Makino, Kawagoe, and Oshita (2011) acquired hyperspectral images of spinaches which were previously inoculated with *E. coli* K-12, and applied artificial neural network (ANN) to predict the actual loads of bacteria. The obtained result was very good (coefficient of determination  $R^2 = 0.97$ , mean square error MSE = 0.038), indicating that hyperspectral imaging had a great potential for real-time safety inspection of packaged fresh vegetables.

Hyperspectral imaging is also found powerful in direct determination of the hygiene of meat, which is more complex in structure and constituents compared to vegetables. Researchers in USDA succeeded in transferring this technique from preliminary laboratory investigations to recent on-line applications in industrial level for detecting faecal contamination and wholesomeness of chicken carcasses (Chao, Yang, & Kim, 2010; Kim, Chen, & Mehl, 2001; Lawrence et al., 2006; Park, Lawrence, Windham, & Smith, 2005; Park, Windham, Lawrence, & Smith, 2004; Yang et al., 2012). Besides, fish freshness was also evaluated using hyperspectral imaging (Menesatti, Costa, Aguzzi, & Sun, 2010). However, to be in accordance with relevant microbiological safety standards and regulations, it is necessary to investigate the potential of hyperspectral imaging for its effectiveness in sensing bacteria especially the pathogenic groups on food matrix. Though publications on HSI for detecting bacteria in meat have been found as illustrated above (Grau et al., 2011; Peng et al., 2011; Tao et al., 2010; Wang et al., 2010), the analyses were all conducted within the short-wavelength near-infrared region, i.e., 400–1100 nm. Therefore, the main objective of the current study was to investigate the potential of hyperspectral imaging in the extended wavelength range of 900–1700 nm for detection the total Enterobacteriaceae loads in raw chicken breast fillets. Specific sub-objectives were: to set up a NIR hyperspectral imaging system covering the spectral range of 900–1700 nm; to establish PLSR calibration models for predicting the loads of Enterobacteriaceae; to evaluate the efficiency of important wavelength selection methods; and to visualise the distribution of Enterobacteriaceae on raw chicken breast fillets.

## 2. Materials and methods

### 2.1. Chicken fillets

Commercially packed fresh chicken breast fillets were purchased from a local supermarket and were transported to the Food Refrigeration and Computerised Food Technology (FRCFT) Laboratory at UCD, Dublin, Ireland within 30 min. These samples were then stored in a refrigerator at  $4 \pm 1^\circ\text{C}$  (temperature range of the refrigerator:

$0\text{--}10^\circ\text{C}$ ) during the course of the study (9 consecutive days). On each day of experiment, one package of chicken breast fillets was taken at random from the fridge to reach room temperature ( $21 \pm 1^\circ\text{C}$ ) for 10–15 min. The fillets were then cut into pieces with an aseptic knife and scissors to form samples with a thickness of approximately 5 mm. The prepared chicken meat pieces were then transferred into individual sterile Petri dishes (90 mm in diameters) aseptically. The surface of each meat piece was flattened by spreading using a T-shaped sterile spreader aiming to acquire a homogeneous distribution of bacteria on the surface and to avoid undesired glitter in subsequently gained images due to sample surface curvature. Prepared samples, each weighing ca. 10 g, were subsequently scanned by a hyperspectral imaging system and their corresponding Enterobacteriaceae loads were determined by traditional microbiological methods.

### 2.2. Acquisition of hyperspectral images

A laboratory-based pushbroom hyperspectral imaging system was set up in reflectance mode to acquire hyperspectral images of the prepared samples. As shown in Fig. 1, the system composes mainly of six components: a translation stage (MSA15R-N, AMT-Linearways, SuperSlides&Bushes Corp., India) driven by a stepper motor (GPL-DZTSA-1000-X, Zolix Instrument Co., China), two 500 W tungsten-halogen illuminating lamps (V-light, Lowell Light Inc., USA), a spectrograph (ImSpector N17E, Spectral Imaging Ltd., Oulu, Finland), a CCD camera (Xeva 992, Xenics Infrared Solutions, Belgium), and a computer with a control software (SpectralCube, Spectral Imaging Ltd., Finland) for image acquisition.

To avoid distortions of images, frame rate and exposure time of the camera and the motor speed were carefully adjusted to achieve a pixel resolution of 0.58 mm both horizontally and vertically. During image acquisition, lids were removed from Petri dishes containing chicken breast fillets and the dishes were put on the translation stage which moved at a speed of approximately  $45\text{ mm s}^{-1}$ . During each scan, a line of light entering into the spectrograph was dispersed and projected onto the CCD array of the camera, where optical signals were then transformed into electronic signals. The acquired two-dimensional signals described the spectral profiles of corresponding pixels in that specific line. By amalgamating the data from scanning lines whose spatial coordinates were previously defined, a three-dimensional image (called hypercube) was obtained, with the first two dimensions accounting for spatial coordinates and the third one for spectral intensities.

Besides acquiring images of the samples, two additional standard images were also acquired for image calibration. The first

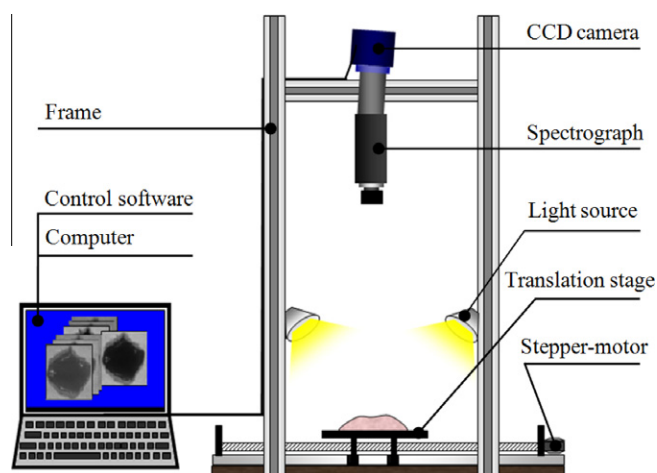


Fig. 1. Schematic diagram showing the set-up of the laboratory-based hyperspectral imaging system in reflectance mode.

image was acquired for a white Teflon tile (ca. 100% reflectance), and the second image to record the dark current (ca. 0% reflectance) of the camera was acquired when the illumination was off and the lens of the camera was entirely covered with its opaque cap.

### 2.3. Determination of Enterobacteriaceae loads

The number of total Enterobacteriaceae in chicken fillets was determined using a pour plate technique (Crowley et al., 2005; Ridell & Korkeala, 1997). Each sample (10 g) was aseptically taken out of the Petri dish and transferred into a stomach bag, where 90 ml sterile buffered peptone water (CM0509, Oxoid, Basingstoke, UK) was subsequently added. Samples were then homogenised in a stomacher (Seward, London, UK) for 2 min. A series of dilutions were made and desired duplicate aliquots (1 ml) were added to sterile Petri dishes and 15–20 ml violet red bile glucose (VRBG) agar (CM0485, Oxoid, Basingstoke, UK) were added. After solidification of the agar an additional 10 ml VRBG medium was overlaid. When solidified the plates were inverted and incubated at 30 °C for 48 h. The growth of colonies was then checked, and those sized above 0.5 mm in diameter and with purple-pink colour and surrounding haloes were considered typical Enterobacteriaceae colonies. Only the plates with Enterobacteriaceae counts between 25 and 250 were considered as valid for further calculation. According to this criterion and by considering possible contamination during experiments, the Enterobacteriaceae loads (in log<sub>10</sub> CFU g<sup>-1</sup>) for 33 samples were finally attained. The obtained data were arranged in ascending order and every third sample (11 in total) was selected for inclusion into an independent prediction set and the remaining 22 samples constituted the calibration set.

### 2.4. Data processing

The flow chart of data processing utilised in this study is presented in Fig. 2. There are three main steps: data preparation (including image calibration, masking, region of interest (ROI) selection and spectrum extraction), model calibration (considering two different spectral ranges and selected wavelengths) and model application (or construction of prediction map).

#### 2.4.1. Image calibration

The acquired hyperspectral images of chicken samples ( $r_{\text{sample}}$ ) should be corrected for stability and easier interpretation (Yao &

Lewis, 2010). The calibrated images ( $R_{\text{sample}}$ ) were calculated using the following formula with the aid of the two standard images obtained as aforementioned:

$$R_{\text{sample}} = \frac{r_{\text{sample}} - r_{\text{dark}}}{r_{\text{white}} - r_{\text{dark}}} \quad (1)$$

where  $r_{\text{white}}$  and  $r_{\text{dark}}$  represent the standard images acquired for the white calibration tile and the dark current of the camera, respectively.

#### 2.4.2. ROI selection

To ensure the quality of spectra which were subsequently used in establishing calibration models, regions of interest (ROIs) were selected manually. An ellipse area containing approximately 1500 pixels was carefully selected on each image within the meat portion. This was done by utilising the drawing tool in ENVI 4.6.1 (ITT Visual Information Solutions, Boulder, CO, USA). The average spectrum was then calculated from the ROI of a calibrated image to stand for the corresponding sample.

#### 2.4.3. Image masking

Masking was conducted on sample images in the prediction set. In this study, band 150 (at 1396 nm) of low reflectance was subtracted from band 15 (at 944 nm) of high reflectance and the resulting image was segmented using an optimal threshold value of 0.25. To remove isolated parts originating from edges of Petri dishes, morphological operations (i.e., image opening) were performed. The created masks were then applied to the calibrated images.

#### 2.4.4. Establishment of calibration models

Spectral profiles usually involve many variables and they tend to be of high multicollinearity. This situation is even worse in hyperspectral images, where huge amount of spatial information is added. Therefore methods are required to reduce the dimension of data and to eliminate redundant information. Partial least squares regression (PLSR) is such a chemometric algorithm that has been widely used in many fields for both qualitative and quantitative analyses (Geladi et al., 2004). PLSR decomposes both predictors  $X$  and dependent variable  $Y$  into several principal components (PCs), where the orthogonal score  $T$  of  $X$  is correlated with  $Y$  (Wold, Sjöström, & Eriksson, 2001) by using the following formulas:

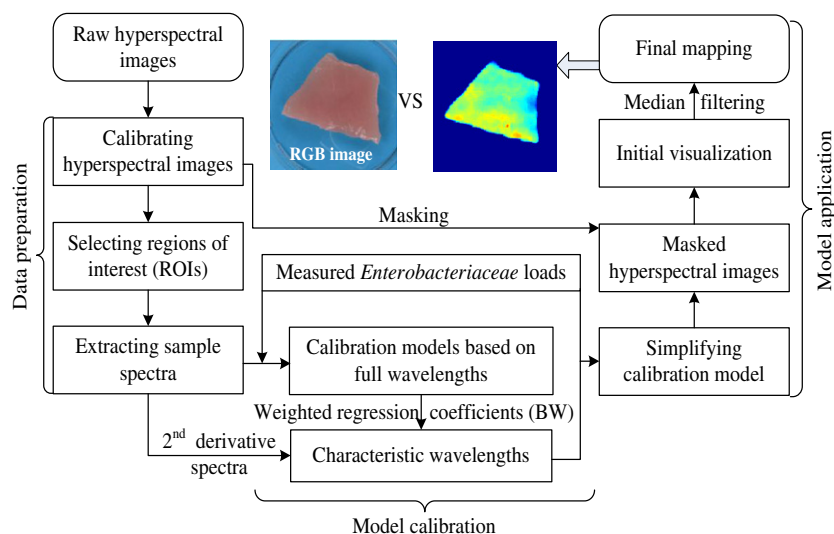


Fig. 2. A schematic diagram showing the data processing routines.

$$\mathbf{Y} = \mathbf{XB} + \mathbf{E} = \mathbf{XW}_a^* \mathbf{C} + \mathbf{E} = \mathbf{TC} + \mathbf{E} \quad (2)$$

$$\mathbf{W}_a^* = \mathbf{W}_a (\mathbf{P}^T \mathbf{W}_a)^{-1} \quad (3)$$

where  $\mathbf{B}$  is the regression coefficients;  $\mathbf{E}$  is a residual error matrix;  $\mathbf{W}_a$  is the PLS weights;  $a$  is the number of latent variables (LVs) adopted;  $\mathbf{P}$  and  $\mathbf{C}$  are loadings for  $\mathbf{X}$  and  $\mathbf{Y}$ , respectively. The selection of the number of latent variables to be used (i.e., the number of PCs) is a critical point in PLS regression. In this study, the optimal number of LVs was determined at the minimum value of the root mean squared error during leave-one-out full cross-validation (RMSECV).

#### 2.4.5. Selection of wavelengths

In general, selecting some important wavelengths is preferred to reduce the high dimensionality of the hyperspectral data, which helps in reducing computing time and also lessens the cost for hardware set-up. Many methods are available for selection of important wavelengths, where allocating pronounced peaks and/or valleys in second derivative spectra (2ndDerS) and weighted PLS regression coefficients (BW) are among the most frequently employed methods (Barbin, Elmasry, Sun, & Allen, 2012; Kamruzzaman, ElMasry, Sun, & Allen, 2012). In this study, the second derivative spectra were gained by applying Norris gap method (Norris & Ritchie, 2008) with a gap size of one. On the other hand, important wavelengths were selected via a BW plot resulting from a PLSR model where spectra were normalised. The selected wavelengths by the above two methods were then used to develop simplified models.

#### 2.4.6. Model application

After a good simplified model was established, it was employed in predicting the bacterial loads of chicken samples in the prediction set. Specifically, the spectra from the masked sample images were subjected to the established model, as a result of which the corresponding bacterial loads at all pixels were gained for each chicken image. The predicted bacterial loads in each mask region were then averaged to represent the final predicted load of Enterobacteriaceae on that chicken fillet.

#### 2.4.7. Model evaluation

Several statistical criteria, i.e., root mean squared errors for calibration, cross-validation as well as prediction (RMSEC, RMSECV and RMSEP, respectively), and coefficients of determination for calibration, cross-validation and prediction ( $R_c^2$ ,  $R_{cv}^2$  and  $R_p^2$ , respectively) were calculated as follows based on the reference and predicted values of the total Enterobacteriaceae counts:

$$\text{RMSE} = \sqrt{\frac{1}{n} \sum_{i=1}^n (y_i - y_{m,i})^2} \quad (4)$$

$$R^2 = 1 - \frac{\sum (y_{m,i} - y_i)^2}{\sum (y_{m,i} - y_{mm})^2} \quad (5)$$

where  $y_i$  and  $y_{m,i}$  are the Enterobacteriaceae loads for sample  $i$  determined by microbiological tests and by PLSR models, respectively;  $y_{mm}$  represents the mean of the reference Enterobacteriaceae counts. It is always expected to obtain RMSEs as close as zero with  $R^2$  as close as one. Specifically, a value of  $R^2$  between 0.82 and 0.90 indicates good performance of a model, while values for  $R^2$  lower than 0.82 or higher than 0.90 reveal imprecise or excellent models, respectively (Williams, 2001).

#### 2.4.8. Visualisation of bacterial distribution

Colour images were created with different colours representing different levels of bacterial loads that were predicted by the optimal simplified model. Thus, by checking the distribution of colours,

one could reach the interesting information about the distribution of Enterobacteriaceae on the meat surfaces, which cannot be accomplished by utilising traditional microbiological methods. To suppress isolated noise and enhance the visualization, a  $5 \times 5$  median filter was employed.

### 3. Results and discussion

#### 3.1. Spectra of chicken breast fillets

After checking the hypercubes, it was found that the images at bands before 930 nm and after 1660 nm were of heavy salt and pepper noise due to the low signal-to-noise ratio in these two spectral regions. Therefore, only spectra within range 930–1660 nm were selected for assays. The spectra of selected samples representing different levels of bacterial loads are shown in Fig. 3. Generally, there are three pronounced absorption peaks in the original reflectance spectra centering at 971, 1191 and 1415 nm. The three peaks can be assigned to O–H second overtone, second overtone of C–H and first overtone of O–H, respectively (Cozzolino & Murray, 2004; Ortiz-Somovilla, España-España, Gaitán-Jurado, Pérez-Aparicio, & De Pedro-Sanz, 2007). More specifically, 971 and 1415 nm are two characteristic bands for water, while 1191 nm is related to fatty acid moieties (Prieto, Roehe, Lavín, Batten, &

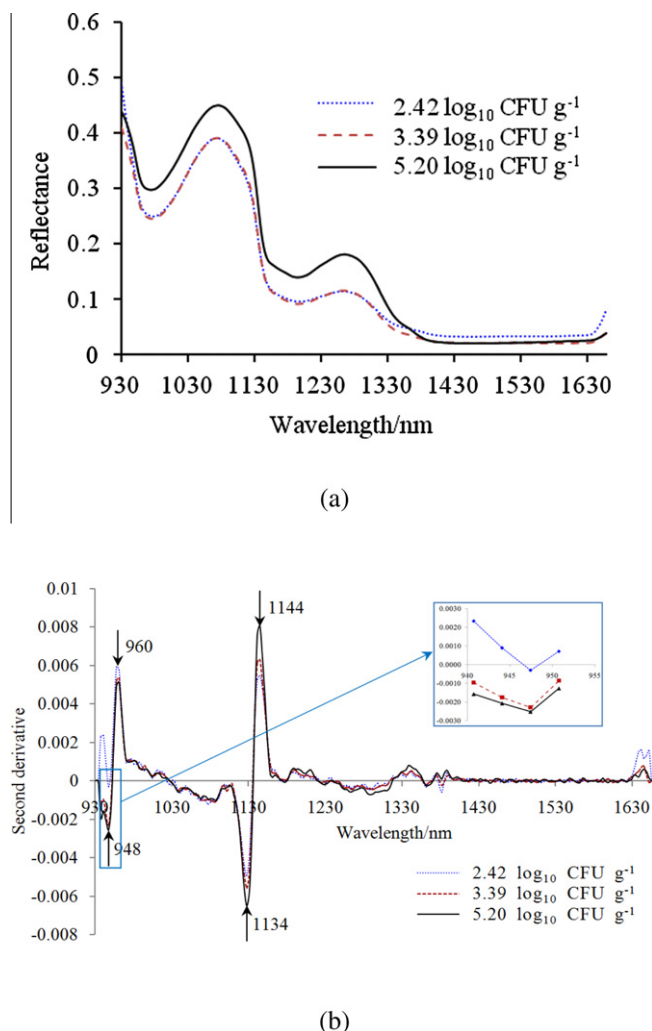


Fig. 3. Spectral profiles of chicken fillets with different amount of total Enterobacteriaceae. (a) Original spectra. (b) Second derivative spectra.



Andrés, 2009; Ritthiruangdej, Ritthiron, Shinzawa, & Ozaki, 2011). It should be noted that in the range of 1450–1635 nm, there were broad absorption bands which showed nearly flat curves in the reflectance spectra. In this spectral region, there are some absorption peaks which can be ascribed to first overtone of C–H combination and first overtone of N–H (Berzaghi, Dalla Zotte, Jansson, & Andrighetto, 2005; Gonzalez-Martin, Gonzalez-Perez, Hernandez-Mendez, & Alvarez-Garcia, 2002; Prieto, Andres, Giraldez, Mantecon, & Lavin, 2006; Shenk, Workman, & Westerhaus, 2008), but these peaks are attenuated or merged due to the predominant presence of water (Brøndum et al., 2000; Kamruzzaman, ElMasry, Sun, & Allen, 2011) which makes up around 69% (w/w) of raw chicken fillets. In addition, it is noticed in Fig. 3(a) that the spectrum of meat with  $5.20 \log_{10} \text{CFU g}^{-1}$  Enterobacteriaceae is substantially different from those with lower loads. This phenomenon is probably due to profound changes of physiochemical parameters in meat over spoilage process (Alexandrakis et al., 2012).

Second derivative transformation is a popular preprocessing method that is commonly used to eliminate background noise, and it is also frequently employed to enhance spectral resolutions (Kirsch & Drennen, 1995; Patel, Luner, & Kemper, 2000). As can be seen in Fig. 3(b), after Norris gap second derivative treatment of the spectra, several feature wavelengths are observed. For example, two strong sharp peaks at 948 and 960 nm were obtained, corresponding to fat and moisture content, respectively (Hoving-Bolink et al., 2005; Ortiz-Somovilla et al., 2007). Besides, two additional wavelengths at 1134 and 1144 nm can be assigned to  $-\text{CH}_3$  stretching second overtone (Dowell, Throne, Wang, & Baker, 1999; Prieto et al., 2009).

### 3.2. Establishment of calibration models

Two models based on full wavelength ranges of 930–1660 and 930–1450 nm were established, where four LVs were optimal and thus were adopted in both cases. The performances of the two models were quite good and similar as shown in Table 1.  $R^2$ ,  $R^2_{\text{CV}}$  and  $R^2_{\text{P}}$  were as high as 0.88, 0.82 and 0.85, respectively, while the errors were no more than  $0.47 \log_{10} \text{CFU g}^{-1}$ . The similarity in model performance implied that the overwhelming majority of chemical information related to the presence of Enterobacteriaceae of different concentrations was located in the spectral range from 930 to 1450 nm. As a result, the spectral range 930–1450 nm was chosen for subsequent analyses.

### 3.3. Simplified models

In the case of the second derivative method, four potential important wavelengths were picked at 948, 960, 1134 and 1144 nm as shown in Fig. 3(b) and they were used to build new simplified PLSR models instead of full wavelengths (Barbin et al., 2012). As shown in Table 1, though not as satisfactory as the full

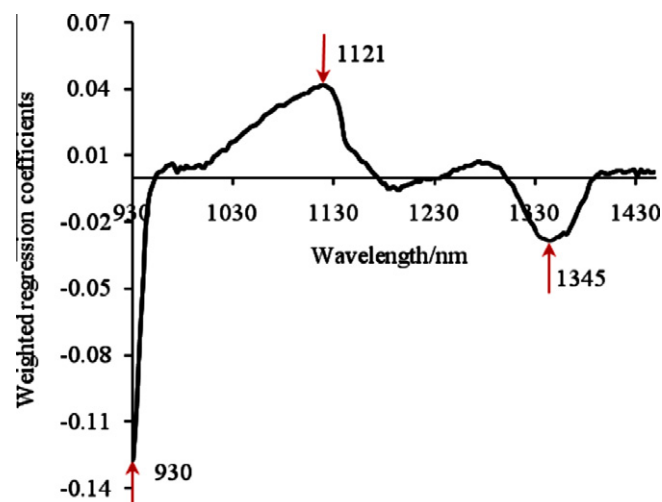


Fig. 4. Plot of weighted regression coefficients for selection of important wavelengths.

wavelength model, the 2ndDerS-based simplified models yielded good results which illustrated that wavelengths selected from second derivative spectra could be used to elucidate the changes in Enterobacteriaceae loads on chicken fillets.

Even better results were obtained by employing the BW-based method, where wavelengths including 930, 1121 and 1345 nm were selected as shown in Fig. 4. By applying this method,  $R^2$ ,  $R^2_{\text{CV}}$  and  $R^2_{\text{P}}$  were increased to 0.89, 0.86 and 0.87, accompanied with RMSEC, RMSECV and RMSEP of 0.33, 0.40 and  $0.45 \log_{10} \text{CFU g}^{-1}$ , respectively. The fact that the BW-PLSR model had better performance in predicting bacterial loads compared with the 2ndDerS-PLSR method was actually anticipated because by considering both spectra and reference values, wavelengths extracted from the predominant peaks in BW plot were indicative for essential correlation between these wavelengths and the parameter under study (bacterial loads). However, in the 2ndDerS-based method, wavelengths were selected regardless of Enterobacteriaceae loads. The changes of reflectance values at these wavelengths were believed to reflect some major factors, not specifically related with the presence of Enterobacteriaceae, that account for the changes in chicken meat during storage. In other words, the wavelengths selected by 2ndDerS-based method were spectrum-featured wavelengths, while the ones picked by the BW-based method were correlation-featured wavelengths, which gave more straightforward explanations to target parameters.

Based on the above results, the combination of wavelengths selected by 2ndDerS and BW methods was investigated. Almost the same  $R^2$  and RMSEs as those produced by the BW-based simplified PLSR model were attained (Table 1). However, since the difference between the BW-PLSR model and the 2ndDerS-BW-PLSR model was not significant, only the three wavelengths (930, 1121 and

Table 1

The performance of calibration models during calibration (C), cross-validation (CV) and prediction (P).

Methods	Wavelengths/nm	$R^2$			RMSEs/ $\log_{10} \text{CFU g}^{-1}$		
		C	CV	P	C	CV	P
PLSR	930–1660	0.88	0.82	0.85	0.35	0.46	0.47
PLSR	930–1450	0.88	0.82	0.85	0.35	0.45	0.47
2ndDerS-PLSR <sup>a</sup>	948, 960, 1134, 1144	0.86	0.82	0.87	0.38	0.45	0.54
BW-PLSR <sup>b</sup>	930, 1121, 1345	0.89	0.86	0.87	0.33	0.40	0.45
2ndDerS-BW-PLSR <sup>c</sup>	930, 948, 960, 1121, 1134, 1144, 1345	0.89	0.86	0.87	0.33	0.40	0.44

<sup>a</sup> PLS regression based on wavelengths selected from second derivative spectra.

<sup>b</sup> PLS regression based on wavelengths selected from weighted PLS regression coefficients.

<sup>c</sup> PLS regression based on wavelengths selected from weighted PLS regression coefficients and second derivative spectra.

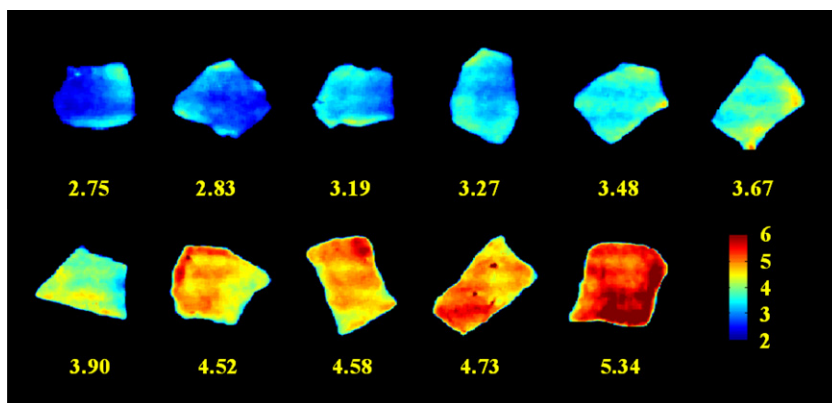


**Fig. 5.** Median-filtered prediction maps for validation set using the simplified PLSR model built on three wavelengths (930, 1121 and 1345 nm) selected from BW. Values under each prediction map of each sample represent predicted Enterobacteriaceae counts (in  $\log_{10}$  CFU  $g^{-1}$ ).

1345 nm) selected by BW–PLSR models should be used in the prediction processes considering model simplicity.

#### 3.4. Visualization of bacterial loads

When the simplified model was finally developed, it was subsequently employed for predicting Enterobacteriaceae loads in each pixel of the image resulting in a new image called the 'prediction map'. Resulting maps from this step are shown in Fig. 5. In the prediction map, a colour scale was provided to describe different microbial loads in each spot of the sample. This means that pixels of larger value in that scale, or equivalently a redder colour, indicates a more intensive existence of microorganisms in such pixels. The black colour represented the background with the remaining variegated portions representing the samples. The average value of all pixels of a sample in the image was also reported in Fig. 5 to display the bacterial load for that corresponding meat sample. As seen in Fig. 5, when the microbial loads increase, the images are generally shifting from blue to reddish, reflecting the growth of bacteria on chicken breast fillets. Moreover, it was noticed that in most of the prediction images, there was comparatively homogeneous distribution of predominant colour(s) in that image. This could be attributed to the somewhat uniform distribution of bacteria on the meat surface, which probably resulted from the efforts of spreading the meat blocks. The spreading operations might also lead to heavier loads at the edges of the sample as could be observed in the prediction maps of some samples. Another reason leading to the phenomenon could be ascribed to the occasional saturation of CCD camera when strong light was reflected from the sample edges.

The ordinary enumeration by microbiological routine work adopted in this paper as a standard method was able to provide an estimation of the Enterobacteriaceae on the whole sample. However, similar bacterial loads can be derived from meat samples with totally different distributions of bacteria, which cannot be identified by the traditional microbiological methods. On the contrary, besides providing the overall estimation of the Enterobacteriaceae load in each sample, the innovative predictive map provided by hyperspectral imaging technique gave clear and useful information about distribution of bacteria, which is very important in food microbiology studies.

#### 4. Conclusions

In this paper, hyperspectral imaging technique was investigated for its effectiveness in non-destructive estimation of Enterobacteriaceae on the surface of raw chicken breast fillets. Precise and stable

PLSR models were built based on full wavelengths with  $R^2 \geq 0.82$  and RMSEs  $\leq 0.47 \log_{10}$  CFU  $g^{-1}$ . Wavelengths were then selected based on second derivative spectra and weighted PLS regression coefficients (BW) and it was demonstrated that the Enterobacteriaceae loads could be accurately predicted by utilising the three wavelengths (930, 1121 and 1345 nm) selected from BW. The prediction map subsequently developed provided a supreme approach for quantitatively visualising the distribution of Enterobacteriaceae on chicken fillets, which can be very useful in determining the sanitation of chicken meat, in understanding bacterial survival and evolution and furthermore in promoting improvements of strategies for reducing bacterial contamination on food matrix. Moreover, apart from the powerful prediction capability, the non-destructive, non-contact and reagentless nature of hyperspectral imaging nominates this technique to be a rapid food safety assessment tool in on-line and at-site inspections, which is greatly favoured in the food industry.

#### Acknowledgements

China Scholarship Council (CSC) and University College Dublin (UCD) are gratefully acknowledged for financial support of this study. Many thanks go to Dr. Zhi-Hang Zhang in FRCFT Group for fruitful discussion and kind help.

#### References

- Alexandrakis, D., Downey, G., & Scannell, A. G. M. (2008). Detection and identification of bacteria in an isolated system with near-infrared spectroscopy and multivariate analysis. *Journal of Agricultural and Food Chemistry*, 56(10), 3431–3437.
- Alexandrakis, D., Downey, G., & Scannell, A. (2012). Rapid non-destructive detection of spoilage of intact chicken breast muscle using near-infrared and Fourier transform mid-infrared spectroscopy and multivariate statistics. *Food and Bioprocess Technology*, 5(1), 338–347.
- Barbin, D., Elmasry, G., Sun, D.-W., & Allen, P. (2012). Near-infrared hyperspectral imaging for grading and classification of pork. *Meat Science*, 90(1), 259–268.
- Berzaghi, P., Dalla Zotte, A., Jansson, L. M., & Andrighetto, I. (2005). Near-infrared reflectance spectroscopy as a method to predict chemical composition of breast meat and discriminate between different n-3 feeding sources. *Poultry Science*, 84(1), 128–136.
- Brøndum, J., Munck, L., Henckel, P., Karlsson, A., Tornberg, E., & Engelsen, S. B. (2000). Prediction of water-holding capacity and composition of porcine meat by comparative spectroscopy. *Meat Science*, 55(2), 177–185.
- Chao, K., Nou, X., Liu, Y., Kim, M., Chan, D., Yang, C., et al. (2008). Detection of fecal/ingesta contaminants on poultry processing equipment surfaces by visible and near-infrared reflectance spectroscopy. *Applied Engineering in Agriculture*, 24(1), 49–55.
- Chao, K., Yang, C.-C., & Kim, M. S. (2010). Spectral line-scan imaging system for high-speed non-destructive wholesomeness inspection of broilers. *Trends in Food Science and Technology*, 21(3), 129–137.
- Cozzolino, D., & Murray, I. (2004). Identification of animal meat muscles by visible and near infrared reflectance spectroscopy. *Lebensmittel-Wissenschaft Und Technologie – Food Science and Technology*, 37(4), 447–452.

- Crowley, H., Cagney, C., Sheridan, J. J., Anderson, W., McDowell, D. A., Blair, I. S., et al. (2005). Enterobacteriaceae in beef products from retail outlets in the Republic of Ireland and comparison of the presence and counts of *E. coli* O157:H7 in these products. *Food Microbiology*, 22(5), 409–414.
- Dowell, F. E., Throne, J., Wang, D., & Baker, J. (1999). Identifying stored-grain insects using near-infrared spectroscopy. *Journal of Economic Entomology*, 92(1), 165–169.
- Du, C. J., & Sun, D. -W. (2006). Learning techniques used in computer vision for food quality evaluation: A review. *Journal of Food Engineering*, 72(1), 39–55.
- Dubois, J., Neil Lewis, E., Fry, J. F. S., & Calvey, E. M. (2005). Bacterial identification by near-infrared chemical imaging of food-specific cards. *Food Microbiology*, 22(6), 577–583.
- ElMasry, G., & Sun, D.-W. (2010). Principles of hyperspectral imaging technology. In D.-W. Sun (Ed.), *Hyperspectral imaging for food quality analysis and control* (pp. 3–43). San Diego: Academic Press.
- Feng, Y. -Z., & Sun, D. -W. (2012). Application of hyperspectral imaging in food safety inspection and control: A review. *Critical Reviews in Food Science and Nutrition*, 52(11), 1039–1058.
- Geladi, P., Sethson, B., Nyström, J., Lillhonga, T., Lestander, T., & Burger, J. (2004). Chemometrics in spectroscopy: Part 2. Examples. *Spectrochimica Acta Part B: Atomic Spectroscopy*, 59(9), 1347–1357.
- Gonzalez-Martin, I., Gonzalez-Perez, C., Hernandez-Mendez, J., & Alvarez-Garcia, N. (2002). Mineral analysis (Fe, Zn, Ca, Na, K) of fresh Iberian pork loin by near infrared reflectance spectrometry: Determination of Fe, Na and K with a remote fibre-optic reflectance probe. *Analytica Chimica Acta*, 468(2), 293–301.
- Gowen, A. A., O'Donnell, C. P., Cullen, P. J., Downey, G., & Frias, J. M. (2007). Hyperspectral imaging: An emerging process analytical tool for food quality and safety control. *Trends in Food Science and Technology*, 18(12), 590–598.
- Grau, R., Sánchez, A. J., Girón, J., Iborra, E., Fuentes, A., & Barat, J. M. (2011). Nondestructive assessment of freshness in packaged sliced chicken breasts using SW-NIR spectroscopy. *Food Research International*, 44(1), 331–337.
- Hoving-Bolink, A. H., Vedder, H. W., Merks, J. W. M., de Klein, W. J. H., Reimert, H. G. M., Frankhuizen, R., et al. (2005). Perspective of NIRS measurements early post mortem for prediction of pork quality. *Meat Science*, 69(3), 417–423.
- Kamruzzaman, M., ElMasry, G., Sun, D.-W., & Allen, P. (2011). Application of NIR hyperspectral imaging for discrimination of lamb muscles. *Journal of Food Engineering*, 104(3), 332–340.
- Kamruzzaman, M., ElMasry, G., Sun, D.-W., & Allen, P. (2012). Prediction of some quality attributes of lamb meat using near-infrared hyperspectral imaging and multivariate analysis. *Analytica Chimica Acta*, 714, 57–67.
- Karimi, Y., Maftoonazad, N., Ramaswamy, H. S., Prasher, S. O., & Marcotte, M. (2012). Application of hyperspectral technique for color classification avocados subjected to different treatments. *Food and Bioprocess Technology*, 5(1), 252–264.
- Kim, M., Chen, Y., & Mehl, P. (2001). Hyperspectral reflectance and fluorescence imaging system for food quality and safety. *Transactions of the American Society of Agricultural Engineers*, 44(3), 721–729.
- Kirsch, J. D., & Drennen, J. K. (1995). Near-infrared spectroscopy: Applications in the analysis of tablets and solid pharmaceutical dosage forms. *Applied Spectroscopy Reviews*, 30(3), 139–174.
- Lawrence, K. C., Windham, W. R., Park, B., Heitschmidt, G. W., Smith, D. P., & Feldner, P. (2006). Partial least squares regression of hyperspectral images for contaminant detection on poultry carcasses. *Journal of Near Infrared Spectroscopy*, 14(4), 223–230.
- Lin, M., Al-Holy, M., Mousavi-Hesary, M., Al-Qadiri, H., Cavinato, A. G., & Rasco, B. A. (2004). Rapid and quantitative detection of the microbial spoilage in chicken meat by diffuse reflectance spectroscopy (600–1100 nm). *Letters in Applied Microbiology*, 39(2), 148–155.
- Liu, F., He, Y., Wang, L., & Sun, G. (2011). Detection of organic acids and pH of fruit vinegars using near-infrared spectroscopy and multivariate calibration. *Food and Bioprocess Technology*, 4(8), 1331–1340.
- Lorente, D., Aleixos, N., Gómez-Sanchis, J., Cubero, S., García-Navarrete, O., & Blasco, J. (2012). Recent advances and applications of hyperspectral imaging for fruit and vegetable quality assessment. *Food and Bioprocess Technology*, 5(4), 1121–1142.
- Menesatti, P., Costa, C., Aguzzi, J., & Sun, D.-W. S. (2010). Quality evaluation of fish by hyperspectral imaging. In D.-W. Sun (Ed.), *Hyperspectral imaging for food quality analysis and control* (pp. 273–294). San Diego: Academic Press.
- Menesatti, P., D'Andrea, S., & Costa, C. (2007). Spectral and thermal imaging for meat quality evaluation. In C. Lazzaroni, S. Gigli, & D. Gabiña (Eds.), *Evaluation of carcass and meat quality in cattle and sheep* (pp. 115–134). Wageningen: Wageningen Academic Publishers.
- Menesatti, P., Zanella, A., D'Andrea, S., Costa, C., Paglia, G., & Pallottino, F. (2009). Supervised multivariate analysis of hyper-spectral NIR images to evaluate the starch index of apples. *Food and Bioprocess Technology*, 2(3), 308–314.
- Norris, K. H., & Ritchie, G. E. (2008). Assuring specificity for a multivariate near-infrared (NIR) calibration: The example of the Chambersburg Shoot-out 2002 data set. *Journal of Pharmaceutical and Biomedical Analysis*, 48(3), 1037–1041.
- Olsson, C., Åhrné, S., Pettersson, B., & Molin, G. (2004). DNA based classification of food associated Enterobacteriaceae previously identified by Biolog GN microplates. *Systematic and Applied Microbiology*, 27(2), 219–228.
- Ortiz-Somovilla, V., España-España, F., Gaitán-Jurado, A. J., Pérez-Aparicio, J., & De Pedro-Sanz, E. J. (2007). Proximate analysis of homogenised and minced mass of pork sausages by NIRS. *Food Chemistry*, 101(3), 1031–1040.
- Park, B., Windham, W. R., Lawrence, K. C., & Smith, D. P. (2004). Hyperspectral image classification for fecal and ingesta identification by spectral angle mapper. In *Transactions of the American society of agricultural engineers. Annual international meeting*. St. Joseph, MI: American Society of Agricultural Engineers.
- Park, B., Lawrence, K., Windham, W., & Smith, D. (2005). Detection of cecal contaminants in visceral cavity of broiler carcasses using hyperspectral imaging. *Applied Engineering in Agriculture*, 21(4), 627–635.
- Patel, A. D., Luner, P. E., & Kemper, M. S. (2000). Quantitative analysis of polymorphs in binary and multi-component powder mixtures by near-infrared reflectance spectroscopy. *International Journal of Pharmaceutics*, 206(1–2), 63–74.
- Peng, Y., Zhang, J., Wang, W., Li, Y., Wu, J., Huang, H., et al. (2011). Potential prediction of the microbial spoilage of beef using spatially resolved hyperspectral scattering profiles. *Journal of Food Engineering*, 102(2), 163–169.
- Prieto, N., Andres, S., Giraldez, F. J., Mantecon, A. R., & Lavin, P. (2006). Potential use of near infrared reflectance spectroscopy (NIRS) for the estimation of chemical composition of oxen meat samples. *Meat Science*, 74(3), 487–496.
- Prieto, N., Roehe, R., Lavin, P., Batten, G., & Andrés, S. (2009). Application of near infrared reflectance spectroscopy to predict meat and meat products quality: A review. *Meat Science*, 83(2), 175–186.
- Ray, B. (2000). *Fundamental food microbiology* (2nd ed.). CRC press.
- Ridell, J., & Korkeala, H. (1997). Minimum growth temperatures of *Hafnia alvei* and other Enterobacteriaceae isolated from refrigerated meat determined with a temperature gradient incubator. *International Journal of Food Microbiology*, 35(3), 287–292.
- Ritthiruangdej, P., Ritthirong, R., Shinzawa, H., & Ozaki, Y. (2011). Non-destructive and rapid analysis of chemical compositions in Thai steamed pork sausages by near-infrared spectroscopy. *Food Chemistry*, 129(2), 684–692.
- Rodriguez-Saona, L. E., Khambaty, F. M., Fry, F. S., & Calvey, E. M. (2001). Rapid detection and identification of bacterial strains by Fourier transform near-infrared spectroscopy. *Journal of Agricultural and Food Chemistry*, 49(2), 574–579.
- Rodriguez-Saona, L. E., Khambaty, F. M., Fry, F. S., Dubois, J., & Calvey, E. M. (2004). Detection and identification of bacteria in a juice matrix with Fourier transform-near infrared spectroscopy and multivariate analysis. *Journal of Food Protection*, 67(11), 2555–2559.
- Shao, Y., Bao, Y., & He, Y. (2011). Visible/near-infrared spectra for linear and nonlinear calibrations: A case to predict soluble solids contents and pH value in peach. *Food and Bioprocess Technology*, 4(8), 1376–1383.
- Shenk, J. S., Workman, J. J., & Westerhaus, M. O. (2008). Application of NIR spectroscopy to agricultural products. In D. A. Burns & E. W. Ciurczak (Eds.), *Handbook of near-infrared analysis* (3rd ed. Boca Raton, Florida, USA: CRC Press.
- Siripatrawan, U., Makino, Y., Kawagoe, Y., & Oshita, S. (2010). Near infrared spectroscopy integrated with chemometrics for rapid detection of *E. coli* ATCC 25922 and *E. coli* K12. *Sensors and Actuators B: Chemical*, 148(2), 366–370.
- Siripatrawan, U., Makino, Y., Kawagoe, Y., & Oshita, S. (2011). Rapid detection of *E. coli* contamination in packaged fresh spinach using hyperspectral imaging. *Talanta*, 85(1), 276–281.
- Sun, D. -W. (1996). Variable geometry ejectors and their applications in ejector refrigeration systems. *Energy*, 21(10), 919–929.
- Sun, D. -W. (1997a). Thermodynamic design data and optimum design maps for absorption refrigeration systems. *Applied Thermal Engineering*, 17(3), 211–221.
- Sun, D. -W. (1997b). Solar powered combined ejector vapour compression cycle for air conditioning and refrigeration. *Energy Conversion and Management*, 38(5), 479–491.
- Sun, D. -W. (1998). Comparison of the performances of NH<sub>3</sub>-H<sub>2</sub>O, NH<sub>3</sub>-LiNO<sub>3</sub> and NH<sub>3</sub>-NaSCN absorption refrigeration systems. *Energy Conversion and Management*, 39(5–6), 357–368.
- Sun, D. -W. (1999). Comparative study of the performance of an ejector refrigeration cycle operating with various refrigerants. *Energy Conversion and Management*, 40(8), 873–884.
- Sun, D. -W. (2000). Inspecting pizza topping percentage and distribution by a computer vision method. *Journal of Food Engineering*, 44(4), 245–249.
- Sun, D. -W., & Eames, I. W. (1996). Performance characteristics of HCFC-123 ejector refrigeration cycles. *International Journal of Energy Research*, 20(10), 871–885.
- Sun, D. -W., & Brosnan, T. (2003). Pizza quality evaluation using computer vision – Part 1 – Pizza base and sauce spread. *Journal of Food Engineering*, 57(1), 81–89.
- Sun, D. -W., Eames, I. W., & Aphornratana, S. (1996). Evaluation of a novel combined ejector-absorption refrigeration cycle. 1. Computer simulation. *International Journal of Refrigeration-Revue Internationale du froid*, 19(3), 172–180.
- Suthiluk, P., Saranwong, S., Kawano, S., Nuthumhum, S., & Satake, T. (2008). Possibility of using near infrared spectroscopy for evaluation of bacterial contamination in shredded cabbage. *International Journal of Food Science and Technology*, 43(1), 160–165.
- Tao, F.-F., Wang, W., Li, Y.-Y., Peng, Y.-K., Wu, J.-H., Shan, J.-J., et al. (2010). A rapid nondestructive measurement method for assessing the total plate count on chilled pork surface. *Spectroscopy and Spectral Analysis*, 30(12), 3405–3409.
- Velusamy, V., Arshak, K., Korostynska, O., Oliwa, K., & Adley, C. (2010). An overview of foodborne pathogen detection: In the perspective of biosensors. *Biotechnology Advances*, 28(2), 232–254.
- Wang, W., Peng, Y.-K., & Zhang, X.-L. (2010). Study on modeling method of total viable count of fresh pork meat based on hyperspectral imaging system. *Spectroscopy and Spectral Analysis*, 30(2), 411–415.
- Williams, P. (2001). Implementation of near-infrared technology. In P. Williams & K. Norris (Eds.), *Near infrared technology in the agriculture and food industries* (2nd ed. Minnesota, USA: American Association of Cereal Chemists.
- Wold, S., Sjöstöm, M., & Eriksson, L. (2001). PLS-regression: A basic tool of chemometrics. *Chemometrics and Intelligent Laboratory Systems*, 58(2), 109–130.

- Woodcock, T., Fagan, C. C., O'Donnell, C. P., & Downey, G. (2008). Application of near and mid-infrared spectroscopy to determine cheese quality and authenticity. *Food and Bioprocess Technology*, 1(2), 117–129.
- Yang, C.-C., Kim, M. S., Kang, S., Cho, B.-K., Chao, K., Lefcourt, A. M., et al. (2012). Red to far-red multispectral fluorescence image fusion for detection of fecal contamination on apples. *Journal of Food Engineering*, 108(2), 312–319.
- Yao, H., & Lewis, D. (2010). Spectral preprocessing and calibration techniques. In D. -W. Sun (Ed.), *Hyperspectral imaging for food quality analysis and control* (pp. 45–78). San Diego: Academic Press.
- Zheng, C. X., Sun, D. -W., & Zheng, L. Y. (2006a). Recent applications of image texture for evaluation of food qualities – A review. *Trends in Food Science & Technology*, 17(3), 113–128.
- Zheng, C. X., Sun, D. -W., & Zheng, L. Y. (2006b). Recent developments and applications of image features for food quality evaluation and inspection – A review. *Trends in Food Science & Technology*, 17(12), 642–655.